Research Square

Preprints are preliminary reports that have not undergone peer review.
They should not be considered conclusive, used to inform clinical practice,
or referenced by the media as validated information.

Fiber metabolite butyrate reduces gp130 by targeting TRAF5 in colorectal cancer cells

Yin Yuan
Zhejiang University School of Medicine First Affiliated Hospital
Bo Li
Zhejiang University School of Medicine First Affiliated Hospital
Yanbin Kuang
Shanghai Jiao Tong University School of Medicine Affiliated Renji Hospital
Shuo Ni
Shanghai Pudong Hospital
Aoxiang Zhuge
Zhejiang University School of Medicine First Affiliated Hospital
Jing Yang
Zhejiang University School of Medicine First Affiliated Hospital
Longxian Lv
Zhejiang University School of Medicine First Affiliated Hospital
Silan Gu
Zhejiang University School of Medicine First Affiliated Hospital
Ren Yan
Zhejiang University School of Medicine First Affiliated Hospital
Yating Li
Zhejiang University School of Medicine First Affiliated Hospital
Kaicen Wang
Zhejiang University School of Medicine First Affiliated Hospital
Liya Yang
Zhejiang University School of Medicine First Affiliated Hospital
Xueling Zhu
Zhejiang University School of Medicine First Affiliated Hospital
Jingjing Wu
Zhejiang University School of Medicine First Affiliated Hospital
Xiaoyuan Bian
Zhejiang University School of Medicine First Affiliated Hospital
Luanjuan Li (✉ ljli@zju.edu.cn)
State Key Laboratory for Diagnosis and Treatment of Infectious Diseases, The First Affiliated Hospital, School of Medicine, Zhejiang University, Hangzhou 310003, China https://orcid.org/0000-0003-0078-

8769

Primary research

Keywords: Colorectal cancer, Sodium butyrate, GP130, TRAF5, protein stability

Posted Date: April 15th, 2020

DOI: https://doi.org/10.21203/rs.3.rs-22775/v1

License: This work is licensed under a Creative Commons Attribution 4.0 International License.
Read Full License

Version of Record: A version of this preprint was published at Cancer Cell International on June 3rd, 2020. See the published version at https://doi.org/10.1186/s12935-020-01305-9.

Abstract

Background: Dietary fibers are effective for Colorectal cancer (CRC) treatment. Interleukin-6 (IL-6) and its adaptors are potential targets for CRC therapy. Butyrate, a metabolite of dietary fiber, is a new, highly safe type of targeted drug.

Methods: In this study, Cell Counting Kit-8 cell viability and wound healing assays, western blot analysis, immunofluorescence staining and xenograft tumor mouse models were used to evaluate the anticancer effect of butyrate and its possible mechanism in vivo and in vitro.

Results: Dietary fibers and sodium butyrate (NaB) decreased CRC burden by decreasing IL-6 receptor gp130 and blocking IL-6/JAK2/STAT3 axis activation in vitro and in vivo. Furthermore, NaB reduced gp130 protein level by regulating its degradation rate via targeting TRAF5.

Conclusions: Fiber metabolite butyrate inhibits CRC development by reducing gp130 via TRAF5.

Background

Colorectal cancer (CRC) is among the most common cancers worldwide(1, 2). Genetic factors, dietary habits, lifestyle and inflammation are related to the occurrence of CRC(3-5). In recent years, the morbidity of CRC has continued to rise, and the age of CRC patients has tended to be younger because of changes in people's dietary habits and dietary structure(6, 7). Although the five-year survival rate of CRC patients has increased significantly because of the extensive application of screening, surgery, chemoradiotherapy and other treatment methods, the sequelae of surgical treatment and side effects caused by chemoradiotherapy render the prognosis of CRC unsatisfactory(8). Therefore, more efficient and safer therapeutic approaches for CRC are needed.

Accumulating evidence indicates that dietary adjustment is an important approach to prevent and treat CRC(9-11). A study by Song et al. found that the consumption of a large amount of dietary fibers can reduce the mortality of CRC patients and confer extra benefits to them(12). After entering the intestinal tract, the gut microbiota decomposed dietary fiber into short-chain fatty acids (SCFAs), including butyric acid, a short-chain fatty acid(13, 14). Butyric acid can inhibit inflammatory reactions and apoptosis and also regulate gut microecology(15). O'Keefe et al. reported that CRC patients lacking butyrate-producing *Clostridium* species in the gut microbiota tended to have poor prognoses, suggesting that butyric acid may be related to the prognosis of CRC(16). In addition, several studies have shown that butyrate can induce the apoptosis and differentiation and inhibit the proliferation of CRC cells. The proposed mechanisms include the functions of butyrate as a histone deacetylase (HDAC) inhibitor and DNA methylation inhibitor and so on(17-19). However, the mechanism by which butyrate prevents and treats CRC has not yet been fully elucidated.

Dysregulation of several key signaling molecules is related to the occurrence and development of CRC, especially Interleukin-6 (IL-6)(20). IL-6 is a multifunctional cytokine whose dysfunction and abnormal

expression often lead to disease(21, 22). Kim et al. revealed that serum IL-6 levels were significantly increased in CRC patients and that serum IL-6 levels were positively correlated with the mortality and prognosis of CRC(23). IL-6 exerts its biological effects by binding with its receptors, the IL-6 α receptor (glycoprotein 80, gp80) and the IL-6 β receptor (glycoprotein 130, gp130)(24). A homodimer composed of IL-6 and gp130 can phosphorylate downstream Janus tyrosine kinases (JAKs), which then activate various downstream transcription factors(25). The IL-6/JAK2/STAT3 pathway was discovered to be constitutively activated in human CRC and significantly related to cancer cell proliferation, invasion and migration(26, 27). Grivennikov et al. found that in CRC mouse models, IL-6 promoted the occurrence of CRC, and genetic knockout of IL-6 or STAT3 suppressed the occurrence of CRC(28). Therefore, blocking the IL-6/JAK2/STAT3 signaling axis and its biological effects may be a therapeutic strategy for CRC.

Tumor necrosis factor receptor-associated factors (TRAFs) is an important kind of intracellular signaling protein, which is involved in the activation of a variety of signaling pathways and the proliferation and apoptosis of tumor cells(29, 30). TRAF5 is a kind of TRAFs, which is proved to be a negative regulator of gp130. Hiroyuki et al. revealed that TRAF5 could constitutively connect to gp130, occupying the binding sites of STAT3, inhibiting the dimerization of gp130, thereby suppressing the activation of IL-6/JAK2/STAT3 signaling(31). Therefore, we consider TRAF5 as a potential target for CRC therapy.

Our previous study showed that dietary fibers metabolite butyrate can significantly inhibit the inflammatory response and the expression of IL-4, IL-6, IL-10 and other inflammatory factors in mouse models of nonalcoholic steatohepatitis(32). Inflammation is closely associated with the initiation and development of CRC(33). Therefore, we speculated that butyrate may function as an anticancer drug by regulating inflammation-related signaling pathways. In this study, we firstly revealed the therapeutic effect of high-fiber diet in inhibiting the progression of CRC in xenograft tumor mice models. Next, we identified butyrate as a major component for CRC treatment. Then, we revealed the role of butyrate in suppressing the development of human CRC cells via blocking the activation of IL-6/JAK2/STAT3 signaling pathway. Furthermore, we found that butyrate exhibited its function by up-regulating TRAF5 level and enhancing the combination between TRAF5 and gp130, thereby reducing the IL-6 receptor gp130. Our results may provide a novel approach for molecular targeted therapy for CRC.

Methods

Cell lines and reagents

The HCT-116 and HT-29 human CRC cell lines were purchased from ATCC (Manassas, VA, USA). RPMI 1640 medium (Gibco, Gaithersburg, MD, USA) supplemented with 10% fetal bovine serum (FBS) and 1% penicillin/streptomycin was used to culture both kinds of cells. Cells were cultured in a 37°C incubator with 5% CO_2. Sodium butyrate (NaB) was purchased from Aladdin (Shanghai, China). Recombinant human IL-6 protein was obtained from R&D Systems (Minneapolis, MN, USA).

Cell viability assay

An enhanced Cell Counting Kit-8 (CCK-8; Beyotime, Shanghai, China) was used to measured cell viabilities. HCT-116 cell and HT-29 cell were cultured in 96-well plates with 0-10 mM NaB at a density of 5000 cells per well for 0-36 hours. Then, CCK-8 assay solution was added to each sample. All cells were incubated for 1.5 hours in the dark. The absorbance was assessed at 450 nm. For each condition, 6 independent biological duplicates were assessed.

EdU cell proliferation assay

The cell proliferative ability was assessed by an EdU cell proliferation kit (Beyotime). According to the instructions, EdU working solution was added to cells pretreated with 5 mM NaB for 24 hours. Then, all samples were cultured in an incubator for 2 hours and fixed for 15 minutes. All cells were stained with EdU and Hoechst 33342. Cells were counted and imaged with an Olympus FSX100 microscope (Olympus, Tokyo, Japan).

Apoptosis assay

Apoptosis was assessed by fluorescence-activated cell sorting (FACS) analysis according to the instructions of the Annexin V-FITC detection kit (KeyGEN BioTECH, Nanjing, China). HCT-116 and HT-29 cells were treated with 5 mM NaB or 10 mM NaB for 24 hours. Then, all cells were collected and incubated with FITC-conjugated Annexin V and propidium iodide (PI) dye. Apoptosis was measured by flow cytometry (BD Biosciences Franklin Lakes, NJ, USA). Results were analyzed with CellQuest software.

Colony formation assay

Cells in logarithmic phase were collected and resuspended in RPMI 1640 medium containing 5 mM NaB. Then, cells were transferred to 6-well plates (400 cells per well) and incubated for 14 days. All media were replaced daily. Then, colonies were fixed for 15 minutes and stained with 1% Giemsa stain solution (Solarbio, Beijing, China) for 30 minutes. All colonies were counted.

Wound healing assay

HCT-116 cell and HT-29 cell were cultured in 12-well plates. At 100% confluence, scratches of equal widths were made in the cell monolayers with sterile 10-μl pipette tips. After washing with PBS, all cells were cultured in FBS-free RPMI 1640 medium containing 5 mM NaB for 24 hours. Images were acquired with an Olympus FSX100 microscope (Olympus). The wound closure percentage was calculated with ImageJ software (USA).

Transwell assay

Transwell chambers (Corning Costar, Cambridge, MA, USA) with 8-μm pores were used for this assay. For the cell migration assay, cells were cultured in FBS-free RPMI 1640 medium overnight and transferred to the upper chambers (10^5 cells per well) the next day. Then medium with 10% FBS and 5 mM NaB was added to lower chambers. 24 hours later, the filter membranes were fixed for 15 minutes after washing

with PBS and stained with 1% Giemsa stain solution for 30 minutes. Then, the cells remaining on the upper surface of membranes (non-migrated cells) were gently removed with cotton swabs. The cells remaining on the lower surface (migrated cells) were counted and imaged. For the cell invasion assay, filter membranes precoated with a 1:6 dilution of Matrigel (BD Bioscience, San Diego, CA, USA) were used instead of uncoated filter membranes. The other steps were performed the same as in the cell migration assay.

Western blot analysis

Cells were collected for protein extraction after treated with 5 mM NaB for 24 hours and then 25 ng/ml IL-6 for 30 minutes. RIPA lysis buffer containing protease and phosphatase inhibitors was used to extract cellular proteins. Proteins were separated by SDS-PAGE and were then transferred to PVDF membranes and probed with specific primary antibodies and secondary antibodies. An enhanced chemiluminescence detection kit (Beyotime) was used to visualize the bands. Antibodies specific for gp80 (sc-373780, 1:100) and gp130 (sc-376280, 1:100) were purchased from Santa Cruz Biotechnology (Dallas, TX, USA). Antibodies specific for STAT3 (#9139, 1:1000), JAK2 (#3230, 1:1000), p-STAT3 (#9145, 1:1000), p-JAK2 (#3771, 1:1000) and TRAF5 (#41658, 1:1000) were obtained from CST (Beverly, MA, USA). The anti-GAPDH antibody (BM1623, 1:1000), anti-β-actin antibody (BM0627, 1:1000), anti-α-tubulin antibody (BM1452, 1:1000), anti-rabbit IgG-HRP antibody (BA1054, 1:5000) and anti-mouse IgG-HRP antibody (BA1050, 1:5000) were purchased from Boster Biological Technology (Wuhan, China).

Protein stability assay

Cells were pretreated with 5 mM NaB for 24 hours. Then, 0.5 hours, 1 hour and 2 hours before cells were collected, 30 μg/ml cycloheximide (CHX; MCE, Monmouth Junction, NJ, USA) was added to all cells to block protein translation. The gp130 protein level was assessed by western blot assay.

TCGA database and analysis

TRAF5 gens were analyzed by GEPIA web tools (http://gepia.cancer-pku.cn/) based on TCGA database.

SCFAs Assay

SCFAs were assessed from fecal samples homogenized in buffers. Suspension was centrifuged and the supernatant was collected for test. A gas chromatography and a fused silica capillary column (Nukon^{TM}, Bellefonte, PA, USA) were used for this assay.

Cell transfection

HT-29 cells were transfected with siRNA using Lipofectamine 3000 (Invitrogen, Carlsbad, CA, USA) according to the instruction. Briefly, cells were seeded in 6-well plates at the density of 2×10^4 cells per well the day before transfection. Then cells were transfected with 20 nM siRNA the next day. All mediums were replaced by culture medium 6 hours after transfection and the transfection efficiency was assessed

by fluorescence microscope after 48 hours. Then transfected HT-29 cells were used for experiments according to protocols. The TRAF5 siRNA kit was purchased from Ribobio (Guangzhou, China).

Immunoprecipitation

For this assay, all cells were lysed in NP-40 buffers and centrifuged at 12000 rpm for 10 minutes. Proteins were immunoprecipitated from supernatants with primary antibodies immobilized on protein G agarose beads overnight at 4 °C. Then all proteins were collected for western blot.

RNA extraction and qRT-PCR

Cells treated with 5 mM NaB for 24 hours and 25 ng/ml IL-6 for 30 minutes were collected for RNA extraction. RNA was extracted with a RNeasy Mini Kit (Qiagen, Valencia, USA) and then reverse transcribed to cDNA. The mRNA expression levels were assessed by a VII A7 real-time PCR system (Applied Biosystems, Foster, CA, USA). The primers were listed in Supplementary file 3: Table S1.

Immunofluorescence

All cells were treated with 5 mM NaB for 24 hours and 25 ng/ml IL-6 for 30 minutes and fixed for 15 minutes and blocked with 5% goat serum for 1 hour. Then, cells were incubated with the anti-p-STAT3 antibody (CST, 1:200) overnight at 4°C and with a Cy3-conjugated secondary antibody (Beyotime, 1:500) for 1 hour the next day. Images were acquired with a Zeiss LSM T-PMT confocal microscope (Zeiss, Jena, Germany).

Mouse xenograft tumor model

All animal experiments were manipulated according to guidelines approved by the Animal Care Committee of Zhejiang University School of Medicine. A total of 10^6 HT-29 cells resuspended in 200 μl FBS-free RPMI 1640 medium were injected into BALB/c athymic nude mice (6-week-old, female) subcutaneously. Tumor volumes were measured every two days. When the tumor volume reached 60-80 mm^3, mice were divided into different groups randomly. For dietary fibers experiments, the low-fiber diet (LFD) group was fed with low fibers food (20% fiber) and the high-fiber diet (HFD) group was fed with high fibers food (70% fiber) for 2 weeks. All diets were purchased from Test Diet (Richmond, IN). After 2 weeks, all animals were sacrificed, and tumor tissues and normal peritumoral tissues were collected. All tissues were frozen in liquid nitrogen and fixed with 4% paraformaldehyde for western blot analysis, hematoxylin and eosin (HE) staining and immunofluorescence staining. For butyrate experiments, the control group was intraperitoneally injected with normal saline every day while the NaB group was intraperitoneally injected with 200 mg/kg NaB. Other steps were performed the same as above.

Statistical analysis

Data were analyzed by SPSS software (Chicago, IL, USA) and GraphPad Prism 7.0 (San Diego, CA, USA). The differences between groups were calculated by ANOVA and Student’s t-test. All data are presented as

the mean ± SEM. P < 0.05 was considered significant.

Results

High-fiber diet inhibits CRC development by producing butyrate in xenograft tumor models

To investigate whether dietary fibers can inhibit tumor development in vivo, low-fiber diet (LFD) and high-fiber diet (HFD) were used to treat xenograft tumor mice (Figure 1A). Both of tumor volume and tumor weight were lower in HFD group than those in LFD group ($p < 0.001$) (Figure 1B-D). These results showed that the development of CRC was inhibited by dietary fibers. SCFAs were metabolites of fibers, so we measured the level of SCFAs in feces. Comparing to LFD group, the fecal level of total SCFAs increased in HFD group ($p < 0.001$) (Figure 1E). Furthermore, we observed a significant increase of fecal butyrate (a main kind of SCFAs) in HFD group ($p < 0.001$) (Figure 1F). To further explore the impact of gut microbiota in fecal butyrate, we gave Abx to SPF mice in order to deplete their gut flora. In the condition of HFD feeding, the fecal butyrate level of Abx-treated mice decreased significantly ($p < 0.001$) (Figure 1G). Together, these results showed that dietary fibers could inhibit the development of CRC and gut microbiota was involved in metabolizing fibers into butyrate.

NaB reduces tumor burden and inhibits JAK2/STAT3 signaling axis activation in vivo

In order to demonstrate whether NaB can inhibit tumor growth in vivo, we established nude mouse xenograft tumor models. The volume and weight of tumors in NaB group mice were significantly lower comparing to those in control group mice ($p < 0.001$) (Figure 2A-C). The HE staining results showed a high level of pathological mitosis (arrow in Figure 2D) but no necrosis in tumor tissues from the control group. However, the tumor tissues from the NaB group exhibited a high number of necrotic areas (Figure 2D). Activation of JAK2/STAT3 signaling axis was found to be closely related to the development of CRC(26). The western blotting results showed that protein levels of p-JAK2 and p-STAT3 in NaB group decreased significantly in both tumor (T) and normal peritumoral (N) tissues ($p < 0.001$) (Figure 2E-F). Immunofluorescence staining of tumor tissues revealed similar results. The protein levels of p-STAT3 protein were significantly lower in tumor tissues from the NaB group than those from the control group (Figure 2G-H). Collectively, NaB could reduce tumor burden and inhibit JAK2/STAT3 signaling axis activation in mouse xenograft tumor models.

NaB inhibits CRC cells proliferation in vitro

Cell proliferative abilities were assessed by several different approaches. First, CCK-8 assays were used to measure cell viabilities of HCT-116 and HT-29 cells. Cell viabilities decreased significantly upon treatment of 5 mM and 10 mM NaB ($p < 0.001$), but not significantly upon 1 mM NaB treatment ($p > 0.05$) (Figure 3A). Next, we measured cell apoptosis by FACS analysis. Neither cell line exhibited significant apoptosis when treated with 5 mM NaB ($p > 0.05$) but did with 10 mM NaB treatment ($p < 0.001$) (Figure 3B). Therefore, we considered 5 mM NaB the optimal concentration to inhibit proliferation of CRC cells because of lower levels of cytotoxicity in vitro. In addition, pretreatment with other kinds of SCFAs

(acetate, propionate and valerate, 0.1mM) did not significantly reduced cell viabilities (Supplementary file 1: Figure S1). Proliferating cell nuclear antigen (PCNA) is a common indicator of cell proliferation. NaB treatment decreased the PCNA protein level ($p < 0.001$) (Figure 3C-D), suggesting that the cell proliferation was inhibited by NaB. The results of the EdU cell proliferation assay showed that EdU-positive cells percentage also decreased among cells treated with NaB ($p < 0.001$) (Figure 3E-F). Collectively, these results showed that the cell proliferative ability can be inhibited by NaB.

NaB inhibits the colony formation, migration and invasion ability of CRC cells

The colony formation ability was evaluated by a colony formation assay. The colony formation ability of both two kinds of cells decreased with NaB treatment ($p < 0.001$) (Figure 4A-B). The migration of CRC cells was evaluated by wound healing assays. Wound closure rates decreased after NaB treatment ($p < 0.001$) (Figure 4C-D). In addition, a Transwell experiment was used to assessed the migration and invasion abilities. Consistent with the results in the wound healing assay, treatment with NaB could inhibit the migration of both lines of cells in the Transwell assay ($p < 0.001$). Similar results were observed in the cell invasion assay. Cell invasion abilities decreased after treated with NaB ($p < 0.001$) (Figure 4E-F). These results showed that NaB could decline the abilities of colony formation, migration and invasion ability in CRC cells.

NaB inhibits the activation of IL-6/JAK2/STAT3 signaling

We further explored the mechanism of NaB effect. Decrease of p-JAK2 and p-STAT3 were found in vivo experiments, indicating that NaB may exhibit its effect by targeting JAK2/STST3 axis. However, the JAK2/STAT3 signaling was not activated in vitro experiment because there was no cytokine in RPMI-1640 medium naturally. Thus IL-6 were added to activate the JAK2/STAT3 signaling. We first measured the total protein level and phosphorylation level of JAK2 and STAT3. The phosphorylation levels of JAK2 and STAT3 were significantly increased in cells stimulated with IL-6 ($p < 0.001$), while pretreatment with NaB for 24 hours could significantly decrease the levels ($p < 0.001$) (Figure 5A-C). We gained similar results in the immunofluorescence assay. Protein level of p-STAT3 increased in cells with IL-6 stimulation, and decreased in cells pretreated with NaB (Figure 5D). These results indicated that NaB can inhibit the IL-6/JAK2/STAT3 signaling activation.

NaB reduces the protein level of gp130 by decreasing its protein stability

To further explore the mechanism by which NaB inhibits the hyperactivation of the IL-6/JAK2/STAT3 signaling, we measured protein levels and gene expression levels of IL-6 receptors gp80 and gp130. The western blotting results showed a decrease in the gp80 protein level in HCT-116 cells treated with NaB ($p < 0.01$) but no change in HT-29 cells ($p > 0.05$). However, the gp130 protein level in both of these groups of cells decreased significantly ($p < 0.001$) (Figure 6A-B). These results suggest that NaB may be a specific inhibitor of gp130. Interestingly, the qRT-PCR results showed no significant change in either the gp80 or gp130 gene expression level in cells upon treatment with either IL-6 or NaB ($p > 0.05$) (Supplementary file 2: Figure S2A-B). Therefore, we concluded that NaB can decrease the protein level of

gp130 but cannot inhibit its gene expression. Next, we measured the protein stability of gp130. After protein translation was blocked by the protein translation inhibitor CHX, all cells were collected at different time points for measurement of their gp130 protein level. The degradation rate of gp130 in both cell lines treated with NaB increased ($p < 0.01$) (Figure 6C-F), indicating that NaB could decrease the protein stability of gp130. In conclusion, these results indicated that NaB can increase the protein degradation rate and reduce the protein stability of gp130.

NaB reduces gp130 protein level by increasing TRAF5

Connection of TRAF5 could weaken the dimerization of gp130, resulting in gp130 dysfunction and inactivation of IL-6/JAK2/STAT3 signaling(31). According to GEPIA web tools based on TCGA database (http://gepia.cancer-pku.cn/), in colon adenocarcinoma (COAD) patients, TRAF5 gene expression was lower in tumor tissues (T) than its in normal tissues (N) (Figure 7A). First, we measured TRAF5 protein level in both HCT-116 and HT-29 cells. NaB treatment increased the protein level of TRAF5 in both HCT-116 cells ($p < 0.05$) and in HT-29 cells ($p < 0.001$) (Figure 7B-C). Next, we detected the interaction of TRAF5 and gp130 by co-immunoprecipitation assay. Notably, we found a connection between TRAF5 and gp130, and this connection was partly enhanced by NaB treatment (Figure 7D). Then HT-29 cells were transfected with siRNA against TRAF5 to further explore the potential mechanism. Surprisingly, we found that NaB could not reduce gp130 protein level and cell viabilities in cells treated with siTRAF5 ($p > 0.05$), but could in cells treated with siCtrl ($p < 0.001$), indicating that TRAF5 knockdown could neutralize the effect of NaB (Figure 7E-G). We hypothesized that by increasing TRAF5 level and enhancing the connection between traf5 and gp130, NaB could disable the biological function of gp130 and accelerate its degradation (Figure 7H).

Discussion

The main objective of this study was to explore the therapeutic effect and potential mechanism of butyrate as a novel inhibitor of gp130 in CRC. First, we found that high-fiber diet can significantly inhibiting CRC development in xenograft tumor mice. By assessing the substance in mice feces, we identified butyrate (a major metabolite of fibers) as a potential component for CRC therapy. In addition, we demonstrated that in specific pathogen free (SPF) immunodeficient mice, gut microbiota was necessary for metabolizing fibers into butyrate. Next, we revealed that butyrate significantly inhibited the proliferation, colony formation and translocation abilities of HCT-116 and HT-29 cells. Butyrate exhibited it function by reducing gp130 level and thus blocking IL-6/JAK2/STAT3 signaling activation. However, butyrate did not significantly impact the gp130 gene expression level in either HCT-116 or HT-29 cells. Therefore, we speculated that butyrate may decrease the gp130 level by regulating the protein degradation and stability of gp130. Through a series of experiments, we confirmed that butyrate reduced gp130 level by increasing the adaptor TRAF5 and enhancing the connection of TRAF5 and gp130. As was found by Hiroyuki et al., combination of TRAF5 and gp130 could inhibit the dimerization of gp130, and suppressing the activation of JAK2/STAT3 signaling(31). Base on the above, we speculated that

butyrate could inhibit the dimerization of gp130 and so as to accelerated its degradation by enhancing TRAF5. These results suggest that butyrate may be a drug useful for targeted CRC therapy.

CRC is a common malignancy related to genetic factors, diet and inflammation.(34, 35) Consumption of huge amounts of fibers results in a low risk of mortality.(12) In this study, we found that high-fiber diet can significantly inhibiting CRC development in xenograft tumor mice in which butyrate was the main component. Moreover, we found that after depleting gut microbiota by using antibiotics, the fecal butyrate level of high-fiber diet mice decreased significantly. Thus, we concluded that gut microbiota was necessary for metabolizing dietary fibers into butyrate.

We further explored the mechanism of how fibers treat and prevent CRC. Dysregulation of key cytokines are important to the initiation and progression of CRC, of particular is the dysregulation of the IL-6 family(36, 37). In the progression of cancer, hyperactivation of JAK2/STAT3 signaling result in and poor prognosis(38, 39). In this study, we confirmed that the major metabolite butyrate significantly inhibited the progression of CRC. Treatment with 5 mM butyrate did not induce significant apoptosis in vitro. Therefore, we considered 5 mM butyrate the optimal and safer concentration for inhibiting CRC cell behaviors in vitro. Butyrate suppressed CRC by decreasing gp130 level and inhibiting hyperactivation of IL-6/JAK2/STAT3 signaling. Furthermore, we found that butyrate did not significantly impact gp80 gene expression or protein levels in either HCT-116 or HT-29 cells. Therefore, we speculated that butyrate may be a specific inhibitor of gp130 instead of gp80. Interestingly, the gp130 gene expression level did not change significantly in either HCT-116 cell or HT-29 cell upon treatment with butyrate, indicating that butyrate cannot inhibit the gene expression of gp130. Therefore, we speculated that butyrate may decrease gp130 protein levels by attenuating gp130 protein stability. Through a series of experiments, we found that butyrate reduced the stability and accelerated the degradation of the gp130 protein by increasing its adaptor TRAF5 and enhancing their connection, thus inhibiting the dimerization of gp130 and accelerating gp130 degradation.

However, a study conducted by Yuan et al. revealed that butyrate inhibited the gene expression of gp80 and the phosphorylation of STAT1 in the human CRC cell lines 228 and RKO. This group also found that butyrate did not impact either the gene expression or protein level of gp130(40). These results are in contrast with ours, and this difference may be due to the heterogeneity of cancer cells(41, 42). Expression of gp80 and gp130 expression differs in different kinds of cells. Therefore, the cellular response to butyrate can also differ. This possibility may be important for scientific research but was not explored in this study. Further experiments are needed to explore this possibility.

In conclusion, we demonstrated butyrate as a novel inhibitor of gp130 by targeting TRAF5. These results may contribute to further exploration of CRC.

Conclusion

Fiber metabolite butyrate inhibits CRC development by reducing gp130 via TRAF5.

List Of Abbreviations

CRC, Colorectal cancer; gp80, Glycoprotein 80; gp130, Glycoprotein 130; IL-6, Interleukin-6; JAK2, Janus tyrosine kinase 2; SCFAs, Short-chain fatty acids; NaB, Sodium butyrate; STAT3, Signal transducer and activator of transcription 3; TRAF5, Tumor necrosis factor receptor-associated factor 5.

Declarations

Ethics approval and consent to participate

All animal experiments were manipulated according to guidelines approved by the Animal Care Committee of Zhejiang University School of Medicine

Consent for publication

Not applicable.

Availability of data and materials

The datasets used and/or analysed during the current study are available from the corresponding author on reasonable request.

Competing interests

The authors declare that they have no competing interests.

Funding

This study was supported by the National Natural Science Foundation of China (81790631, 81570512, 81703430), the National Key Research and Development Program of China (2018YFC2000500) and Natural Science Foundation of Zhejiang Province, China (LQ19H030007).

Authors' contributions

LJL, YBK and SN designed the study. YY and BL performed the experiments and drafted the manuscript. JY, AXZG, JFX analyzed the data. LXL, SLG, RY, YTL, KCW, LYY and XYB gave the technical and material support. LJL revised the paper. All authors read and approved the final manuscript.

Acknowledgments

We are grateful to Dr. Jiong Yu, Dr. Yehong Zhang, Dr. Jinlin Chen and Dr. Pei Zhang (The First Affiliated Hospital, School of Medicine, Zhejiang University, Hangzhou, China) for their help in using fluorescence and confocal microscopes.

References

1. Dekker E, Tanis PJ, Vleugels JLA, Kasi PM, Wallace MB. Colorectal cancer. Lancet. 2019;394(10207):1467-80.
2. Siegel RL, Miller KD, Fedewa SA, Ahnen DJ, Meester RGS, Barzi A, et al. Colorectal cancer statistics, 2017. CA Cancer J Clin. 2017;67(3):177-93.
3. Carr PR, Weigl K, Jansen L, Walter V, Erben V, Chang-Claude J, et al. Healthy Lifestyle Factors Associated With Lower Risk of Colorectal Cancer Irrespective of Genetic Risk. Gastroenterology. 2018;155(6).
4. Tabung FK, Liu L, Wang W, Fung TT, Wu K, Smith-Warner SA, et al. Association of Dietary Inflammatory Potential With Colorectal Cancer Risk in Men and Women. JAMA Oncol. 2018;4(3):366-73.
5. Schoen RE, Razzak A, Yu KJ, Berndt SI, Firl K, Riley TL, et al. Incidence and mortality of colorectal cancer in individuals with a family history of colorectal cancer. Gastroenterology. 2015;149(6).
6. Murphy CC, Singal AG, Baron JA, Sandler RS. Decrease in Incidence of Young-Onset Colorectal Cancer Before Recent Increase. Gastroenterology. 2018;155(6).
7. Stoffel EM, Murphy CC. Epidemiology and Mechanisms of the Increasing Incidence of Colon and Rectal Cancers in Young Adults. Gastroenterology. 2020;158(2):341-53.
8. Brenner H, Kloor M, Pox CP. Colorectal cancer. Lancet. 2014;383(9927):1490-502.
9. Dimitrov BD. Fibre and colorectal cancer. Lancet. 1996;348(9032):958-9.
10. Ben Q, Sun Y, Chai R, Qian A, Xu B, Yuan Y. Dietary fiber intake reduces risk for colorectal adenoma: a meta-analysis. Gastroenterology. 2014;146(3).
11. Song M, Garrett WS, Chan AT. Nutrients, foods, and colorectal cancer prevention. Gastroenterology. 2015;148(6).
12. Song M, Wu K, Meyerhardt JA, Ogino S, Wang M, Fuchs CS, et al. Fiber Intake and Survival After Colorectal Cancer Diagnosis. JAMA Oncol. 2018;4(1):71-9.
13. Koh A, De Vadder F, Kovatcheva-Datchary P, Bäckhed F. From Dietary Fiber to Host Physiology: Short-Chain Fatty Acids as Key Bacterial Metabolites. Cell. 2016;165(6):1332-45.
14. Donohoe DR, Holley D, Collins LB, Montgomery SA, Whitmore AC, Hillhouse A, et al. A gnotobiotic mouse model demonstrates that dietary fiber protects against colorectal tumorigenesis in a microbiota- and butyrate-dependent manner. Cancer Discov. 2014;4(12):1387-97.
15. Sivaprakasam S, Prasad PD, Singh N. Benefits of short-chain fatty acids and their receptors in inflammation and carcinogenesis. Pharmacol Ther. 2016;164:144-51.
16. O'Keefe SJD. Diet, microorganisms and their metabolites, and colon cancer. Nat Rev Gastroenterol Hepatol. 2016;13(12):691-706.
17. Sun X, Zhu M-J. Butyrate Inhibits Indices of Colorectal Carcinogenesis via Enhancing α-Ketoglutarate-Dependent DNA Demethylation of Mismatch Repair Genes. Mol Nutr Food Res. 2018;62(10):e1700932.

18. Sebastián C, Mostoslavsky R. Untangling the fiber yarn: butyrate feeds Warburg to suppress colorectal cancer. Cancer Discov. 2014;4(12):1368-70.
19. Thangaraju M, Cresci GA, Liu K, Ananth S, Gnanaprakasam JP, Browning DD, et al. GPR109A is a G-protein-coupled receptor for the bacterial fermentation product butyrate and functions as a tumor suppressor in colon. Cancer Res. 2009;69(7):2826-32.
20. West NR, McCuaig S, Franchini F, Powrie F. Emerging cytokine networks in colorectal cancer. Nat Rev Immunol. 2015;15(10):615-29.
21. Jones SA, Jenkins BJ. Recent insights into targeting the IL-6 cytokine family in inflammatory diseases and cancer. Nat Rev Immunol. 2018;18(12):773-89.
22. Howlett M, Giraud AS, Lescesen H, Jackson CB, Kalantzis A, Van Driel IR, et al. The interleukin-6 family cytokine interleukin-11 regulates homeostatic epithelial cell turnover and promotes gastric tumor development. Gastroenterology. 2009;136(3):967-77.
23. Kim S, Keku TO, Martin C, Galanko J, Woosley JT, Schroeder JC, et al. Circulating levels of inflammatory cytokines and risk of colorectal adenomas. Cancer Res. 2008;68(1):323-8.
24. Murakami M, Hibi M, Nakagawa N, Nakagawa T, Yasukawa K, Yamanishi K, et al. IL-6-induced homodimerization of gp130 and associated activation of a tyrosine kinase. Science. 1993;260(5115):1808-10.
25. Zhang C, Xin H, Zhang W, Yazaki PJ, Zhang Z, Le K, et al. CD5 Binds to Interleukin-6 and Induces a Feed-Forward Loop with the Transcription Factor STAT3 in B Cells to Promote Cancer. Immunity. 2016;44(4):913-23.
26. Johnson DE, O'Keefe RA, Grandis JR. Targeting the IL-6/JAK/STAT3 signalling axis in cancer. Nat Rev Clin Oncol. 2018;15(4):234-48.
27. Yu H, Pardoll D, Jove R. STATs in cancer inflammation and immunity: a leading role for STAT3. Nat Rev Cancer. 2009;9(11):798-809.
28. Grivennikov S, Karin E, Terzic J, Mucida D, Yu G-Y, Vallabhapurapu S, et al. IL-6 and Stat3 are required for survival of intestinal epithelial cells and development of colitis-associated cancer. Cancer Cell. 2009;15(2):103-13.
29. Chen H, Li M, Campbell RA, Burkhardt K, Zhu D, Li SG, et al. Interference with nuclear factor kappa B and c-Jun NH2-terminal kinase signaling by TRAF6C small interfering RNA inhibits myeloma cell proliferation and enhances apoptosis. Oncogene. 2006;25(49):6520-7.
30. Zhu S, Jin J, Gokhale S, Lu AM, Shan H, Feng J, et al. Genetic Alterations of TRAF Proteins in Human Cancers. Front Immunol. 2018;9:2111.
31. Nagashima H, Okuyama Y, Asao A, Kawabe T, Yamaki S, Nakano H, et al. The adaptor TRAF5 limits the differentiation of inflammatory CD4(+) T cells by antagonizing signaling via the receptor for IL-6. Nat Immunol. 2014;15(5):449-56.
32. Ye J, Lv L, Wu W, Li Y, Shi D, Fang D, et al. Butyrate Protects Mice Against Methionine-Choline-Deficient Diet-Induced Non-alcoholic Steatohepatitis by Improving Gut Barrier Function, Attenuating Inflammation and Reducing Endotoxin Levels. Front Microbiol. 2018;9:1967.

33. Lasry A, Zinger A, Ben-Neriah Y. Inflammatory networks underlying colorectal cancer. Nat Immunol. 2016;17(3):230-40.
34. Keum N, Giovannucci E. Global burden of colorectal cancer: emerging trends, risk factors and prevention strategies. Nat Rev Gastroenterol Hepatol. 2019;16(12):713-32.
35. Kastrinos F, Samadder NJ, Burt RW. Use of Family History and Genetic Testing to Determine Risk of Colorectal Cancer. Gastroenterology. 2020;158(2):389-403.
36. Hurtado CG, Wan F, Housseau F, Sears CL. Roles for Interleukin 17 and Adaptive Immunity in Pathogenesis of Colorectal Cancer. Gastroenterology. 2018;155(6):1706-15.
37. Flint TR, Janowitz T, Connell CM, Roberts EW, Denton AE, Coll AP, et al. Tumor-Induced IL-6 Reprograms Host Metabolism to Suppress Anti-tumor Immunity. Cell Metab. 2016;24(5):672-84.
38. Kim H, Kim D, Choi SA, Kim CR, Oh SK, Pyo KE, et al. KDM3A histone demethylase functions as an essential factor for activation of JAK2-STAT3 signaling pathway. Proc Natl Acad Sci USA. 2018;115(46):11766-71.
39. Kusaba T, Nakayama T, Yamazumi K, Yakata Y, Yoshizaki A, Inoue K, et al. Activation of STAT3 is a marker of poor prognosis in human colorectal cancer. Oncol Rep. 2006;15(6):1445-51.
40. Yuan H, Liddle FJ, Mahajan S, Frank DA. IL-6-induced survival of colorectal carcinoma cells is inhibited by butyrate through down-regulation of the IL-6 receptor. Carcinogenesis. 2004;25(11):2247-55.
41. Punt CJA, Koopman M, Vermeulen L. From tumour heterogeneity to advances in precision treatment of colorectal cancer. Nat Rev Clin Oncol. 2017;14(4):235-46.
42. Roerink SF, Sasaki N, Lee-Six H, Young MD, Alexandrov LB, Behjati S, et al. Intra-tumour diversification in colorectal cancer at the single-cell level. Nature. 2018;556(7702):457-62.

Figures

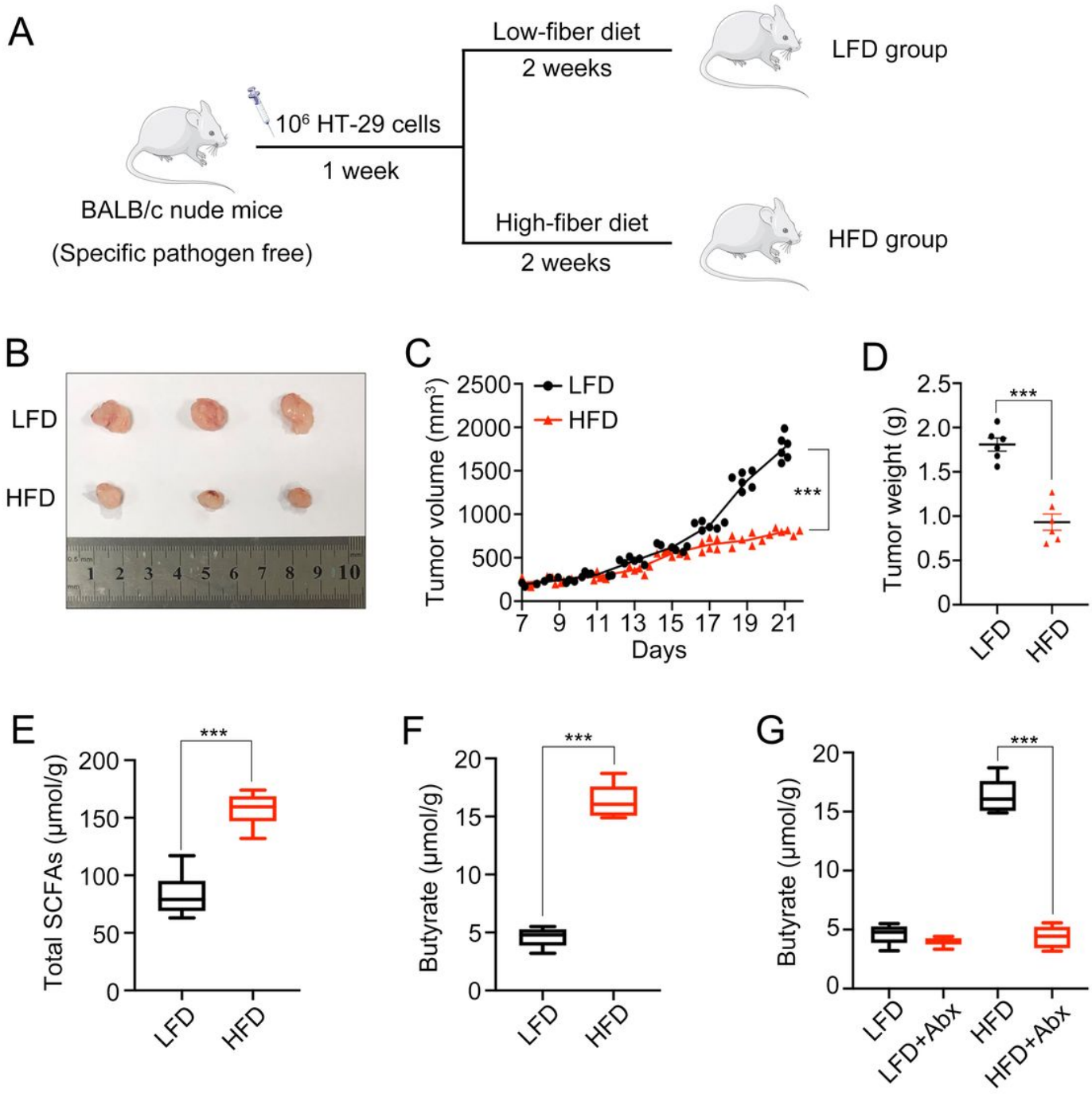

Figure 1

High-fiber diet (HFD) inhibited CRC development. a Protocols of dietary fibers experiments. b-d Images, volumes and weights of tumors. e-f Concentration of total SCFAs and butyrate in fecal samples. g Concentration of fecal butyrate in mice treated with or without antibiotics (Abx). (***, $p < 0.001$)

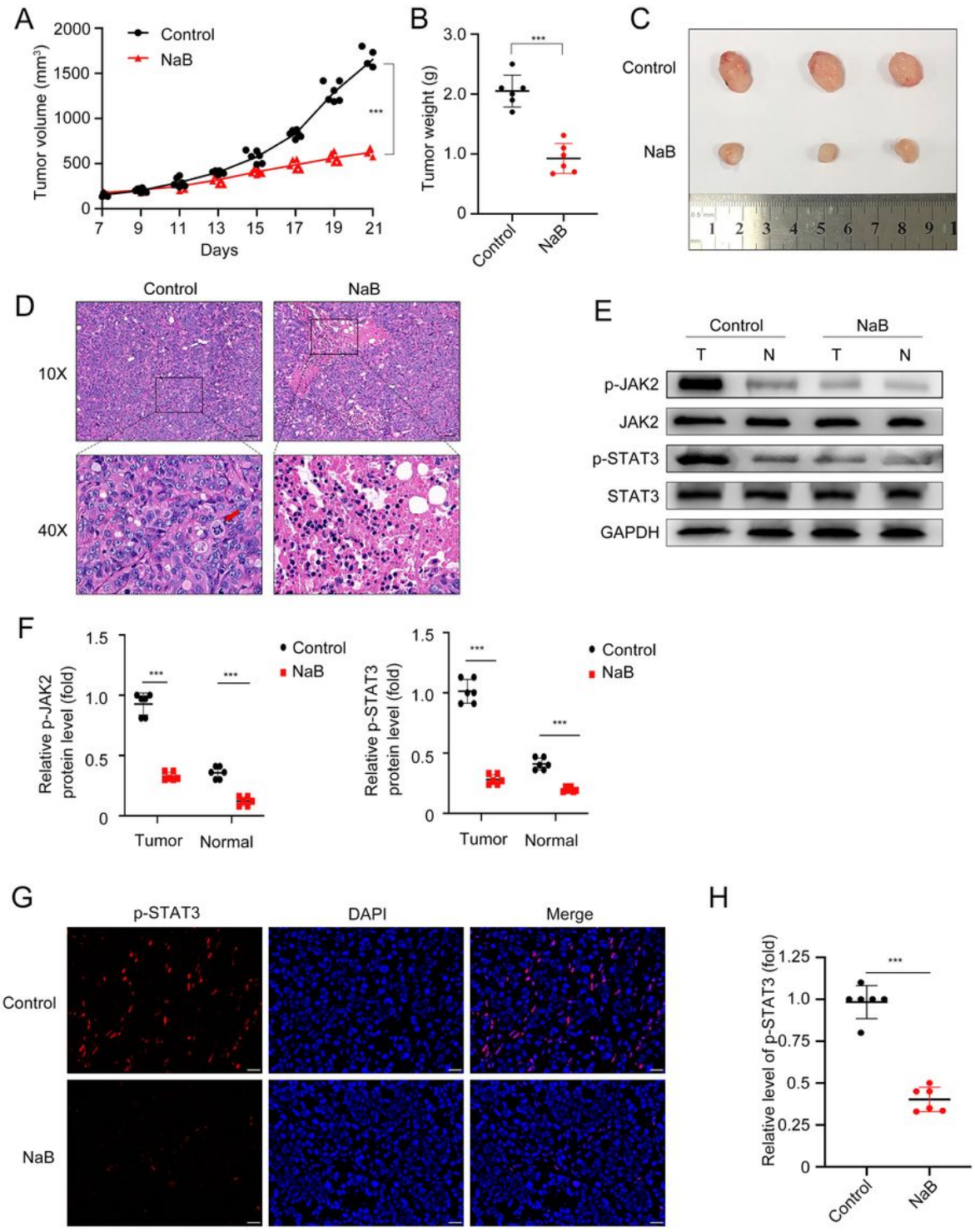

Figure 2

Sodium butyrate (NaB) reduced HT-29 xenograft tumor burden in vivo. a-c Images, volumes and weights of tumors. d HE staining of tumor tissues. The arrow indicates pathological mitosis. Scale bar represents 50 μm. e-f Western blotting of p-JAK2, and p-STAT3 protein levels in tumor tissues (T) and normal peritumoral tissues (N) from mice. g-h Immunofluorescence staining specific for p-STAT3 proteins in mouse tumor tissues. Scale bar represents 20 μm. (***, $p < 0.001$)

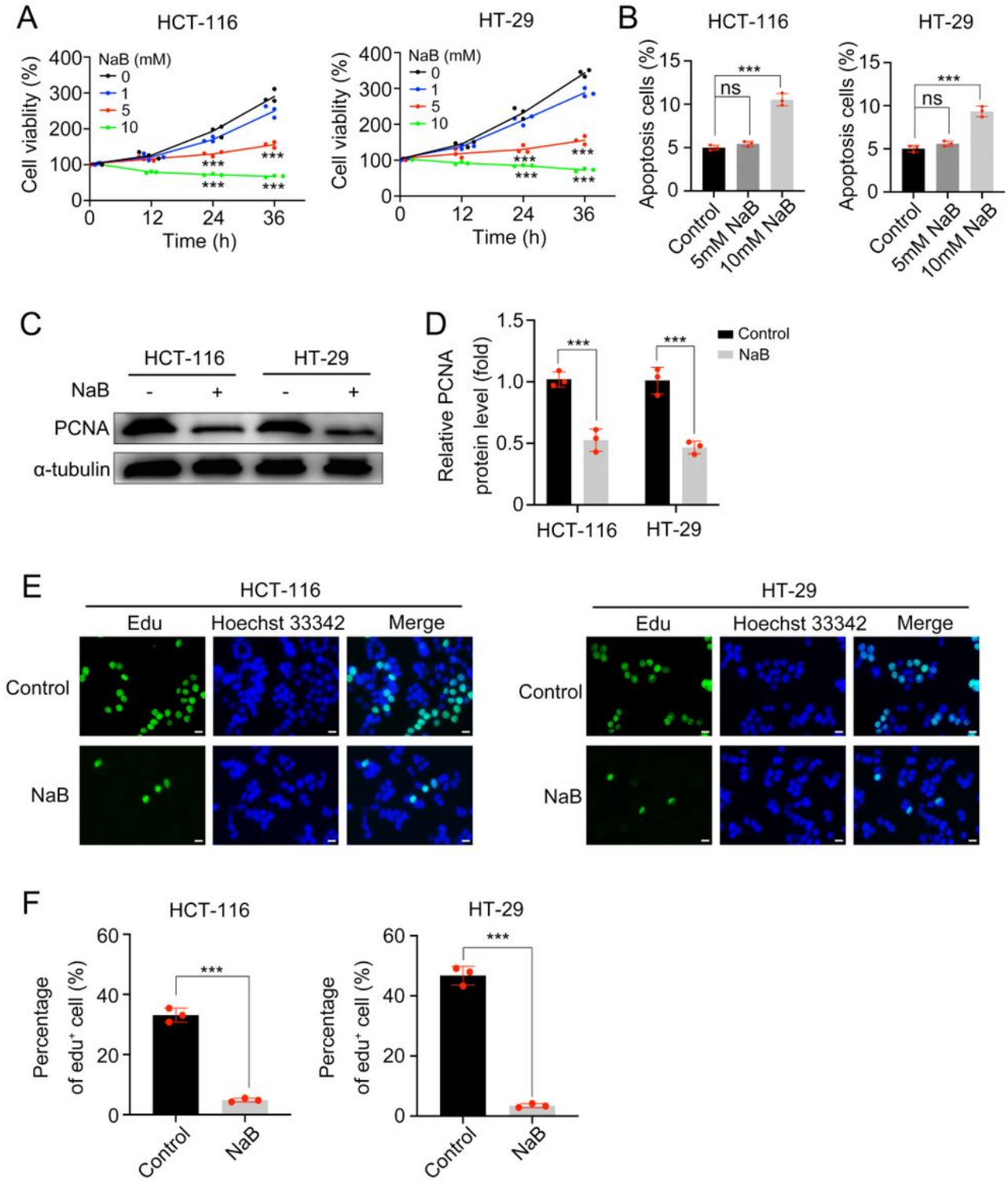

Figure 3

NaB inhibited proliferation of HCT-116 and HT-29 cells. a Cell viabilities of HCT-116 and HT-29 cells treated with 0-10 mM NaB for 0-36 hours. b Cell apoptosis of HCT-116 and HT-29 cells treated with 5 and 10 mM NaB for 24 hours. c-d Western blot analysis of PCNA protein levels in HCT-116 and HT-29 cells treated with 5 mM NaB for 24 hours. e-f Images and percentages of EdU positive cells. Scale bar represents 10 μm. (***, $p < 0.001$; ns: not significant)

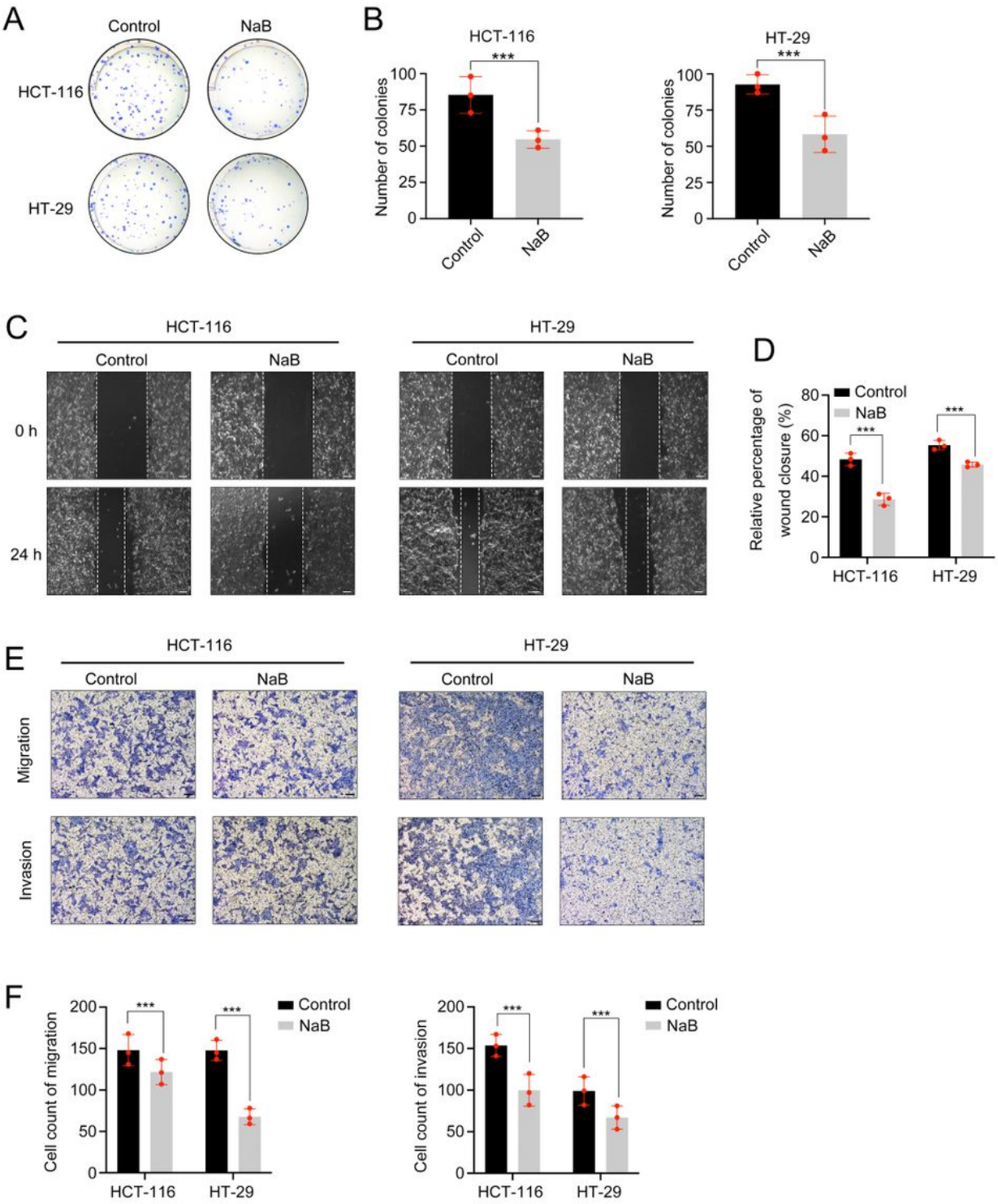

Figure 4

NaB inhibited cell colony formation and translocation. a-b Images and amounts of HCT-116 and HT-29 cell colonies treated with 5 mM NaB for 2 weeks. c-d Wound healing percentage of HCT-116 and HT-29 cells treated with 5 mM NaB for 24 hours. Scale bar represents 100 μm. e-f Images and counts of migrated and invaded cells assessed by Transwell. Scale bar represents 100 μm. (***, $p < 0.001$)

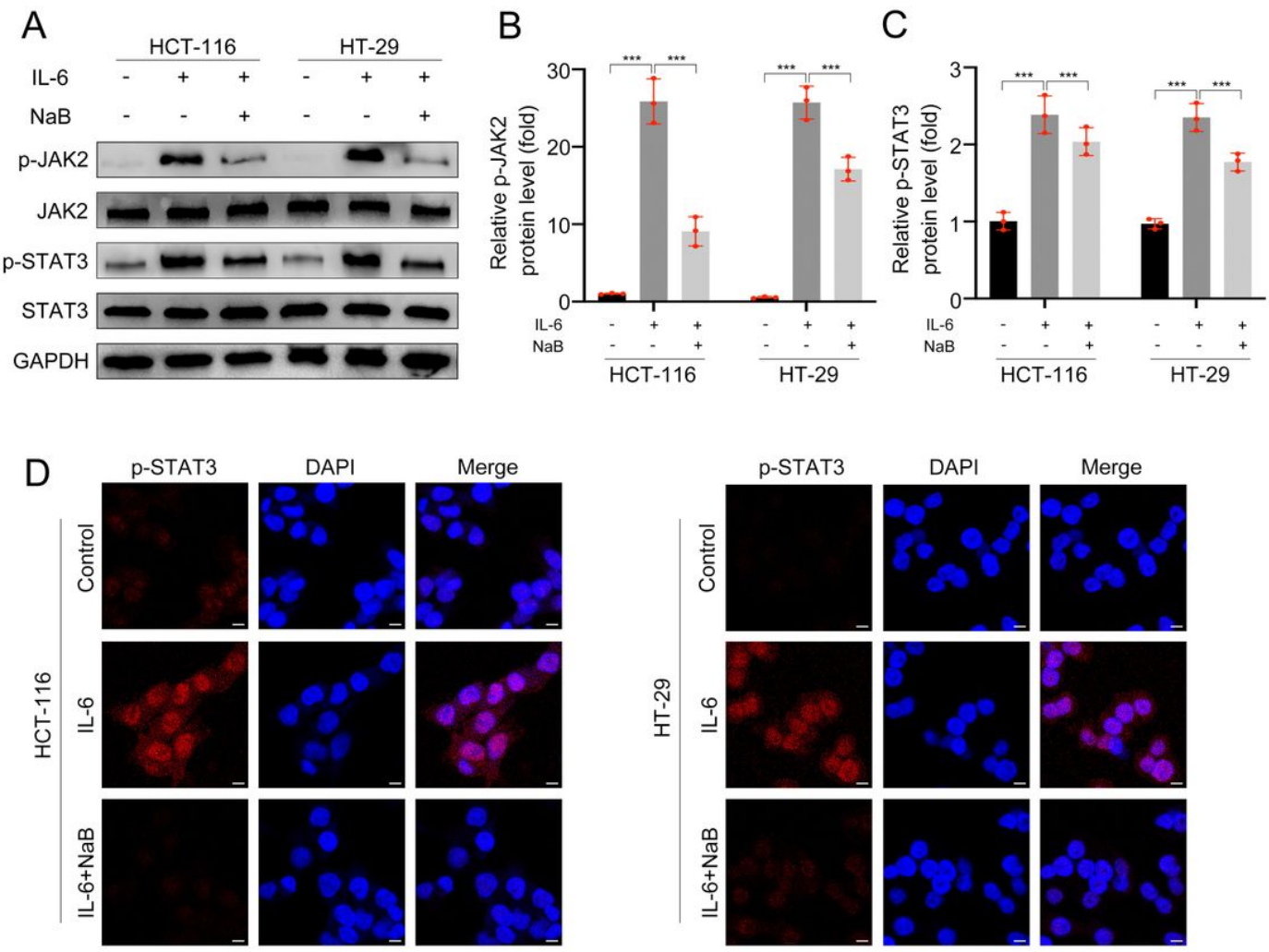

Figure 5

NaB inhibited the activation of IL-6/JAK2/STAT3 signaling pathway. a-c Western blot analysis of p-JAK2, JAK2, p-STAT3, STAT3 protein levels of cells treated with NaB (5 mM) for 24 hours and IL-6 (25 ng/ml) for 30 minutes. d Immunostaining for p-STAT3 (red) and DAPI (blue) of cells pretreated with or without NaB (5 mM) for 24 hours and IL-6 (25 ng/ml) for 30 minutes. Scale bar represents 10 μm. (***, $p < 0.001$)

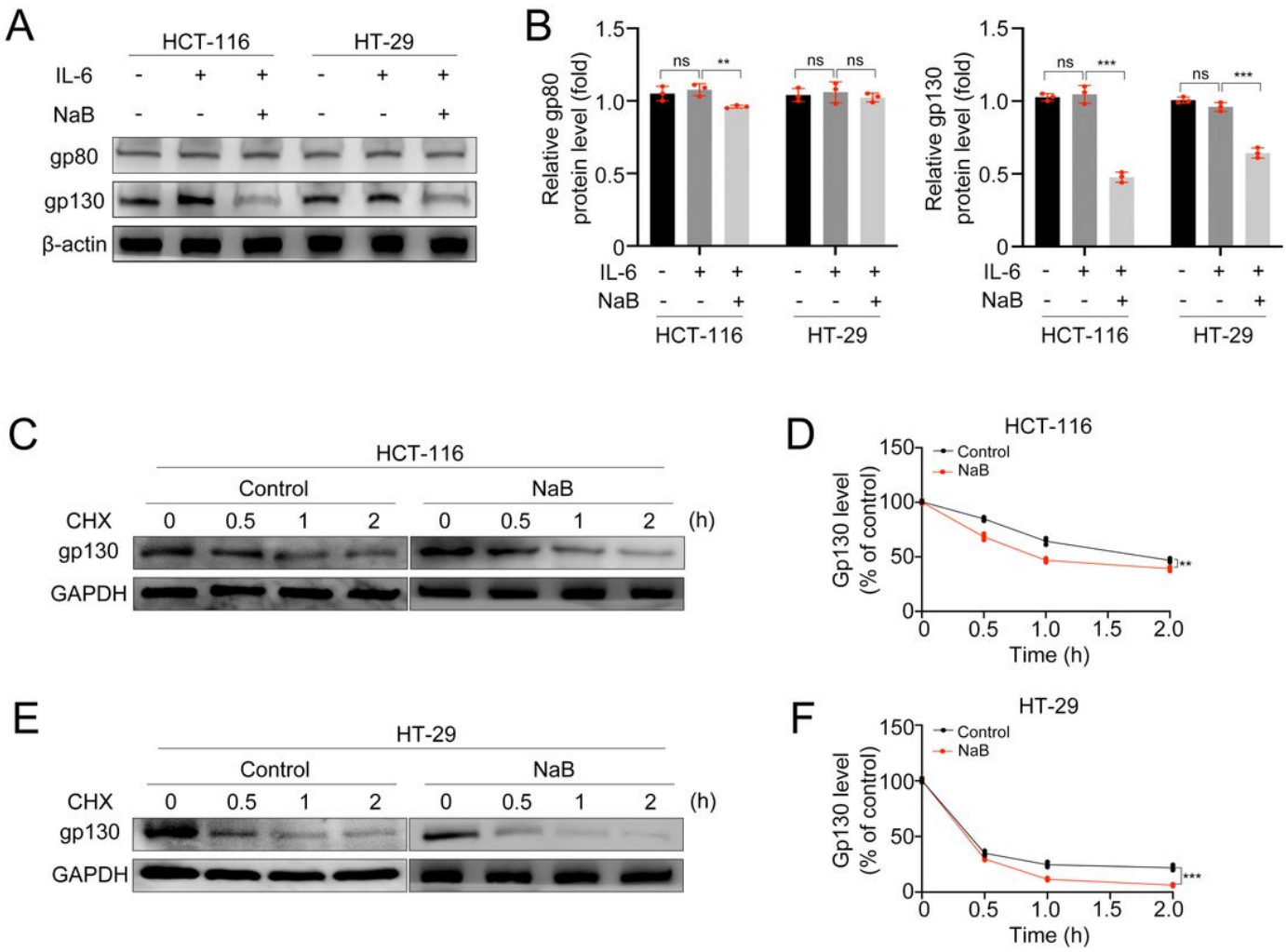

Figure 6

NaB decreased IL-6 receptor gp130 by accelerating its degradation. a-b Western blot analysis of gp80 and gp130 protein levels. c-f Western blotting of gp130 protein levels in cells treated with NaB (5 mM) for 24 hours and CHX (30 μg/ml) for 0, 0.5, 1, 2 hours. (**, $p < 0.01$; ***, $p < 0.001$; ns: not significant)

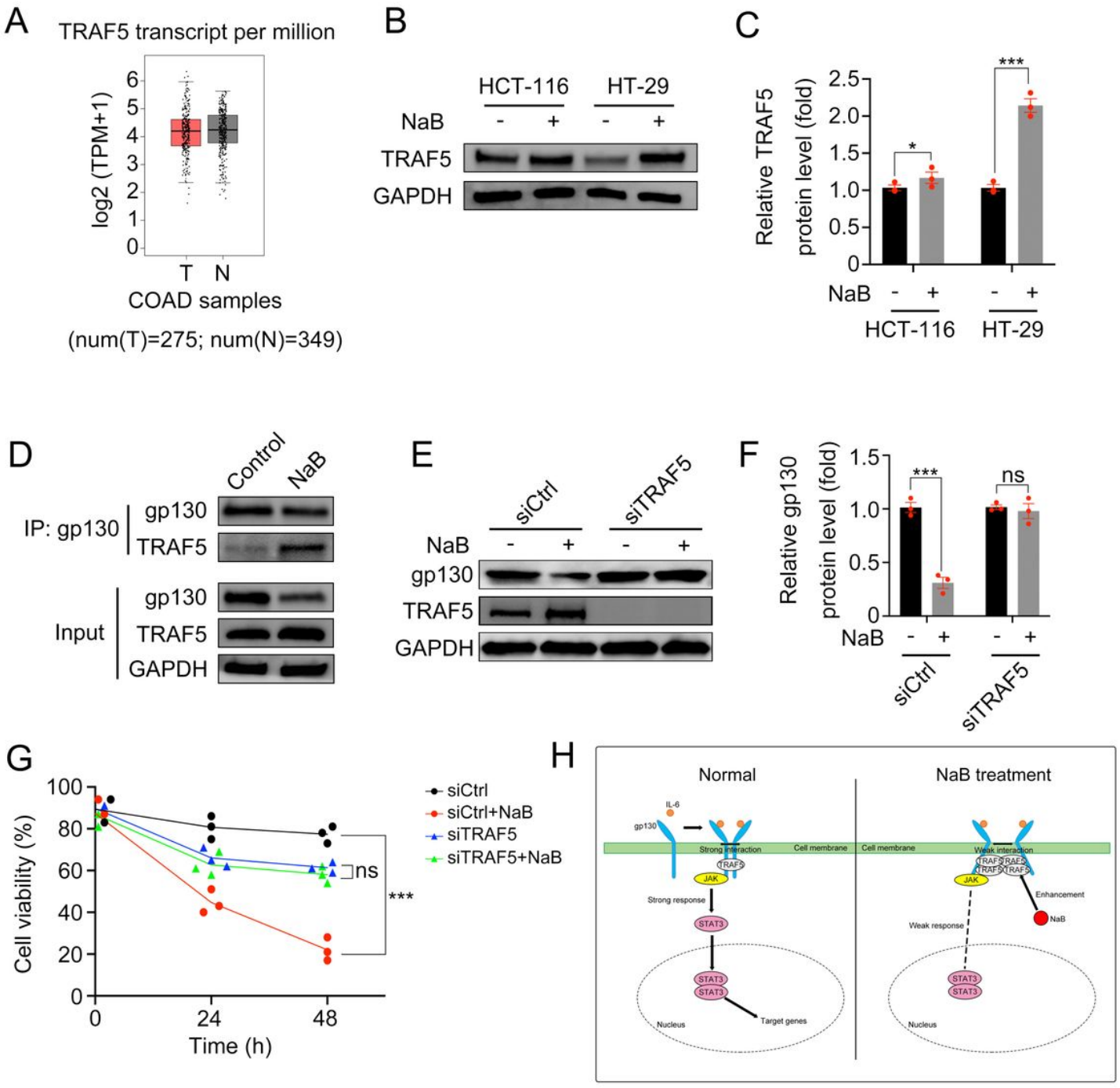

Figure 7

NaB accelerated gp130 degradation by increasing TRAF5. a TRAF5 transcription analyzed by the GEPIA web tool. b-c Western blotting of TRAF5 protein levels in cells treated with NaB (5 mM) for 24 hours. d Co-immunoprecipitation assay of gp130 and TRAF5 in HT-29 cells treated with 5 mM NaB for 24 hours. e-g Rescue experiments of HT-29 cells transfected with TRAF5 siRNA. h A schematic diagram of the mechanism.

Supplementary Files

This is a list of supplementary files associated with this preprint. Click to download.

- figures1.tif
- figures2.tif
- tables1.docx